Salmonella infection leads to severe intestinal inflammation and increased CD4+FoxP3+ Treg cells in streptozotocin-induced hyperglycemic mice

SHANLONG ZHANG[1,2], MEIXIANG WANG[3], XUEMEI WANG[2], HELOU LI[2], HUA TANG[3,4] and XIAOJUN LI[1]

[1]Institute of Clinical Laboratory Science, Jinling Hospital, Southern Medical University, Nanjing, Jiangsu 210002;
[2]Department of Clinical Laboratory, Affiliated Hospital of Taishan Medical University, Taian, Shandong 271000;
[3]Shanghai Public Health Clinical Center, Fudan University, Shanghai 200000; [4]Institute of Immunology,
Taishan Medical University, Taian, Shandong 271000, P.R. China

Abstract. Hyperglycemia promotes the growth and reproduction of bacteria, thereby increasing the probability of infection, which also causes rebound hyperglycemia. Therefore, the interactions of infection and hyperglycemia lead to the progression and deterioration of these diseases. Type 1 diabetes mellitus (T1DM) is an autoimmune disease. Studies have shown that regulatory T cells (Tregs) play a key role in maintaining islet-specific tolerance. Treg deficiency may lead to the development of early pancreatitis and T1DM, and sufficient amounts of Tregs can restore this tolerance, thereby inhibiting the occurrence of T1DM. Moreover, different subpopulations of dendritic cells (DCs) play an important role in activating autoreactive T cells and inducing autoimmune tolerance to autoantigens, which are closely related to the functional diversity caused by different phenotypes, maturation status, and the immune microenvironment of DC subpopulations. In the present study, we used streptozotocin-induced hyperglycemic mice to model T1DM and induced a *Salmonella* infection in the mouse model, leading to aggravated inflammation, which resulted in an elevated proportion of CD103+CD11b+ DCs and a significantly elevated proportion of CD4+FoxP3+ Tregs in the intestinal lamina propria. After co-culturing CD4+ T cells and DCs, we found that CD103+CD11b+ DCs could significantly promote the proliferation of CD4+ T cells. The elevated proportions of CD4+FoxP3+ Tregs were considered to be correlated with the increased number of CD103+CD11b+ DCs.

Introduction

Diabetes is an important risk factor for nosocomial infections. It is difficult to control diabetes after a concurrent infection. The two disorders influence each other and aggravate the disease, leading to high mortality (1). The intestinal mucosal immune system is the first line of defense against intestinal pathogens and external antigen infections, and the system plays a key role in establishing and maintaining homeostasis between the host and the external environment (2). The intestinal mucosal immune system has unique immune cells, including regulatory T cells and tolerant dendritic cells (DCs), and the expression of unique pattern recognition receptors plays a key role in maintaining intestinal tolerance to oral antigens and intestinal commensal bacteria (3). *Salmonella* is one of the main pathogens that causes diarrhea, and its pathogenicity is mainly through the invasion of and replication in host cells (4). Therefore, studying the mechanism of intestinal immune system resistance to *Salmonella* under hyperglycemia may provide new strategies for diabetic patients to resist intestinal pathogen infection.

The main function of regulatory T cells (Tregs) is to suppress or modulate the immune response, and these cells constitute a key part of peripheral immunomodulation (5). Evidence has shown that a lack of Treg regulation plays a role in many autoimmune diseases. One previous study showed that patients with type 1 diabetes mellitus (T1DM) have lower levels of FoxP3+ Tregs (labeled as CD4+CD25+ T cells) than individuals without diabetes (6). However, Tregs are labeled based on low CD127 expression and positive FoxP3 expression. The total number of FoxP3+ Tregs in T1DM patients is the same as in the general population (7). FoxP3+ Tregs are not a simple cell population with common phenotypes but rather a heterogeneous mixture of cell populations with different phenotypic subtypes, which represent the maturation, differentiation, and activation status of cells, or cells in an inhibited state due to different methods or targeted effects. In this way, T1DM may involve changes in

Correspondence to: Dr Xiaojun Li, Institute of Clinical Laboratory Science, Jinling Hospital, Southern Medical University, 305 Zhongshan Road, Nanjing, Jiangsu 210002, P.R. China
E-mail: xiaojunli62@126.com

Dr Hua Tang, Shanghai Public Health Clinical Center, Fudan University, 2901 Caolong Road, Shanghai 200000, P.R. China
E-mail: tanghuazhang218@163.com

the number and balance of Treg subpopulations. One previous study showed that individuals with T1DM have fewer FoxP3^{+} Tregs than individuals without diabetes (8).

A previous study showed that DC subpopulations are involved in the pathogenesis of multiple autoimmune diseases, including T1DM. In peripheral tissues, interactions between DCs and self-reactive effector cells (Th0 cells) induce hyperglycemia in T1DM patients (9). DCs induce the differentiation of autoreactive T cells into pro-inflammatory effector cells to cause the death of islet beta cells, thereby preventing the biosynthesis of insulin. In general, DCs participate in the maintenance of central and peripheral immune tolerance by eliminating autoreactive T cells and inducing Treg production. However, the changes in Tregs at the site of tissue injury and kinetics and phenotypic changes of DCs that occur during the induction of Treg changes have not been established (10).

In the present study, the elevation of the Treg proportion in the intestinal lamina propria (LP) suggested that Tregs play an important role in maintaining intestinal homeostasis after infection in hyperglycemic mice. One possible reason was that the uptake of antigens by CD103^{+}CD11b^{+} DCs in the LP stimulated the proliferation of antigen-specific CD4^{+} T cells and induced differentiation into FoxP3^{+} Tregs. These findings may aid in the development of an in-depth understanding of the T1DM cytological basis, which may provide a theoretical basis for developing systems of T1DM immunotherapy and better clinical application of immune cells.

Materials and methods

Animals. A total of 20 female C57BL/6 (H-2 Kb) mice (6-8 weeks of age, weighing ~18-22 g) were purchased from Vital River (Beijing, China). These animals were maintained in specific pathogen-free conditions at a controlled temperature (18˚C to 20˚C) and humidity (40-70%) with a 12 h light cycle, and access to standard diet and tap water *ad libitum*. This study was approved by the Laboratory Animal Care Committee of Taishan Medical University (Taian, China), and all animal experiments were conducted in accordance with the Guidelines of the Care and Use of Laboratory Animals of Taishan Medical University. These mice were allocated into 4 groups (5 mice in each group): naïve, without any treatment; naïve+S.T., treated with only *Salmonella typhimurium*; streptozotocin (STZ), treated with only STZ; STZ+S.T., treated with STZ and *Salmonella typhimurium*.

Induction of diabetes. STZ-induced T1DM was established by subcutaneous administration with STZ [freshly prepared in citrate buffer; Sigma-Aldrich/Merck KGaA (Darmstadt, Germany)] at a dosage of 200 mg/kg body weight in 10 mice (11). Diabetes/hyperglycemia was confirmed by testing the blood glucose level using a OneTouch® glucose monitoring system (LifeScan Inc., Milpitas, CA, USA).

Infection with Salmonella typhimurium. A single colony of *Salmonella typhimurium* used for infecting the mouse model was inoculated onto an LB agar plate with inoculum and incubated at 37˚C for 12 h. A single colony was then selected and further incubated in LB liquid medium at 37˚C for another 12 h. One hundred microliters of the bacterial broth was transferred to a new test tube containing LB liquid medium and further incubated at 37˚C for 12 h. After diluting the bacterial broth into multiple proportions and agar plate inoculation, the bacterial cultures were incubated at 37˚C for 12 h, followed by calculating the number of bacteria (CFU). Five C57BL/6 mice in the naïve and STZ groups were weighed and orally administered 1x10^{8} CFU *Salmonella typhimurium* (12).

Tissue sectioning and staining. Intestinal and pancreatic tissues were fixed with 10% formaldehyde for 12-24 h at room temperature. The tissues were then paraffin-embedded and cut into 5 μm thick longitudinal sections, and stained with hematoxylin solution for 3 min, eosin solution for 2 min at room temperature, and observed under a light microscope (magnification, x200; Olympus Corporation, Tokyo Japan).

Measurement of cytokines. A total of 0.3 ml blood was collected from the mouse submandibular vein plexus without anticoagulation, and the serum was isolated. In brief, blood samples were refrigerated at 4˚C for 1 h, and centrifuged at 1,000 x g, at 4˚C for 5 min to collect the blood serum. Cytokines, including IL-6 (cat. no. ab100712, Abcam, Cambridge, UK) and interferon γ (IFN-γ; cat. no. ab100689; Abcam) in the serum, were assayed by standard sandwich ELISA in 96-well plates using a capture and detection method, as per the manufacturer's instructions.

Intestinal single cell preparation. Each mouse was euthanized by cervical dislocation to dissect the small intestine. The contents of the small intestine were then flushed by enema and the lamina propria (LP) and mesenteric lymph node (MLN) were removed. IEL medium and ethylenediaminetetraacetic acid (EDTA) washing solution were used for irrigation and rinsing on a shaker at 170 rpm at 37˚C for 40 min. The suspension was filtered twice through a 30-mesh filter. The small intestine was cut into small pieces and incubated with 5 ml type IV collagenase on a shaker at 150 rpm at 37˚C for 40 min. MACS buffer was then added to stop the digestion, and the mixture was passed through an oversized sieve for filtering and homogenization. MACS buffer was also used to rinse the filter to prevent cells from drying out, followed by centrifugation in 45% Percoll medium at 1,800 x g for 10 min at 23˚C and the supernatant was removed. MACS buffer was used to resuspend the tissue pellet, which was filtered through a 40 μm filter and further centrifuged at 1,800 x g for 5 min at 4˚C to discard the supernatant and the cell pellet was resuspended in a final volume of 100 μl RPMI-1640 medium (Gibco, Thermo Fisher Scientific, Inc., Waltham, MA, USA).

Flow cytometry. For cell surface staining, after blocking with 2.4G2 (cat. no. sc-18867; Santa Cruz Biotechnology, Inc., Dallas, TX, USA) at 37˚C for 20 min, cells were stained with diluted (1:200) anti-CD11c-percp-cy5.5 (cat. no. 03212-70; Biogems International, Inc., Westlake Village, CA, USA), anti-MHC Class II IA + IE (cat. no. ab93561; Abcam), anti-CD64-APC (cat. no. 139305; BioLegend, Inc., San Diego, CA, USA), anti-F4/80-FITC (cat. no. 123108; BioLegend, Inc.), anti-PD-L1-PE (cat. no. 124308; BioLegend, Inc.), anti-CD8a (cat. no. 17-0081-82; eBioscience; Thermo Fisher Scientific, Inc.), anti-CD11b-PE (cat. no. 101207; BioLegend, Inc.),

anti-Ly6C-e450 (cat. no. 48-5932-82; eBioscience; Thermo Fisher Scientific, Inc.), anti-NK1.1-Biotin (cat. no. 85-13-5941-85; eBioscience; Thermo Fisher Scientific, Inc.), and anti-CD3e-Biotin (cat. no. 13-0031-86; eBioscience; Thermo Fisher Scientific, Inc.) monoclonal antibodies to analyze DCs, macrophages, monocytes, and neutrophils. For cell counting, stained cells were collected by centrifuging at 140 x g for 5 min at 4˚C, and then quantified by flow cytometry. Phenotypic analysis and cell counts were performed on a BD FACS Aria II Flow Cytometer (BD Bioscience, San Jose, CA, USA) and analyzed using FlowJo 7.6.1 (FlowJo LLC, Ashland, OR, USA).

Reverse transcription quantitative-PCR (RT-qPCR). First, RNA was extracted from the intestinal tissue in mice using TRIzol® (cat. no. 15596-018; Invitrogen; Thermo Fisher Scientific, Inc.). Next, aliquots of each RNA sample (1 μg) were reverse transcribed to produce cDNA using a Quanti-Tect Reverse Transcription kit (Qiagen GmbH, Hilden, Germany). RT-qPCR was performed with a Rotor-Gene SYBR Green PCR Kit (Qiagen GmbH) on a Rotor-Gene Q cycler (Qiagen GmbH). The reaction system (25 μl) included 12.5 μl Rotor-Gene SYBR Green RT-PCR Master Mix (2X), 1 μmol/l PCR forward primers, 1 μmol/l PCR reverse primers, 0.25 μl Rotor-Gene RT Mix, 1 μl RNA (50 ng) and nuclease-free water. A Rotor Gene 6000 thermal circulator (Qiagen GmbH) was used to reverse transcribe mRNA at 55˚C for 10 min. For qPCR, the mixture was then heated at 95˚C for 5 min to activate the Hot Star Taq Plus DNA polymerase. PCR was carried out by the two-step method (denatured at 95˚C for 5 sec, then annealed and extended at 60˚C for 10 sec). Samples were analyzed in triplicate, and experiments were performed at least three times. FoxP3 used glyceraldehyde-phosphate dehydrogenase (GAPDH) as the internal reference. The $2^{-\Delta\Delta Cq}$ method (13) was used to calculate the ratio of gene expression in the experimental group relative to that in the control group with the using the quantification cycles (Cq) as presented in the following formula: $\Delta\Delta Cq = \Delta Cq_{\text{the experimental group}} - \Delta Cq_{\text{the control group}}$, and $\Delta Cq = Cq_{\text{(target gene)}} - Cq_{\text{(internal reference)}}$. FoxP3 primer sequences were as follows: forward sequence, 5'-CCTGGTTGTGAGAAGGTCTTCG-3'; reverse sequence, 5'-TGCTCCAGAGACTGCACCACTT-3'. GAPDH primer sequences were as follows: forward sequence, 5'-AATGGATTTGGACGCATTGGT-3'; reverse sequence, 5'-TTTGCACTGGTACGTGTTGAT-3'. GAPDH expression was used as the internal reference gene.

Statistical analysis. Data are represented as the mean ± standard error of the mean (SEM) or standard deviation (SD). Statistical analyses were performed using GraphPad PRISM 8.0.2.263 (GraphPad Software, La Jolla, CA, USA) by one-way analysis of variance (ANOVA) followed by Dunnett's post hoc tests. Pearson correlation analysis was used to analyze the relationship between CD103+CD11b+ DC cells and CD4+FoxP3+ Tregs. P<0.05 was considered to indicate a statistically significant difference.

Results

Hyperglycemic mice infected with Salmonella typhimurium display increased inflammatory progression and mortality.
After C57BL/6 inbred mice were fasted for 8 h, the mice were weighed and intraperitoneally injected with 200 mg/kg STZ solution. After 72 h, caudal vein blood was collected from each mouse to measure the blood glucose concentration, which was significantly higher in the experimental group (>20 mmol/) than that noted in the control group (Fig. 1A). The body weights of all of the mice were continuously monitored. The body weight of the mice after STZ injection was significantly reduced (Fig. 1A). After STZ injection, the mice showed symptoms, such as polydipsia and polyuria, which were similar to the clinical symptoms of T1DM patients.

Next, we randomly divided the C57BL/6 inbred mice into two groups: the naïve group and the naïve+S.T. group. The STZ-induced hyperglycemic mice were also randomly divided into two groups: the STZ group and the STZ+S.T. group. Animals in the two groups of mice with *Salmonella* infection were orally administered and infected with 1x10⁸ CFU *Salmonella typhimurium* according to the methods described in a previous study (14). The results showed that the two groups of mice infected with *Salmonella typhimurium* (+S.T.) had significantly lower body weights than the naïve group and the STZ group (Fig. 1B). In addition, comparing the mortality between the mice in the naïve+S.T. group and the STZ+S.T. group, hyperglycemic mice with *Salmonella* infection died earlier than mice in the STZ group (Fig. 1B). The hyperglycemic mice with *Salmonella* infection began to die on day 6 post infection and all mice were dead on day 7 after *Salmonella* infection. The C57BL/6 inbred mice with *Salmonella* infection (mice in the naïve+S.T. group) were all dead on day 8 after *Salmonella* infection (Fig. 1B), suggesting that hyperglycemia aggravated *Salmonella* infection and promoted the progression of the disease. ELISA assessment of IFN-γ concentration in mouse serum 3 days after *Salmonella* infection showed significantly higher serum IFN-γ concentrations in the naïve+S.T. group and the STZ+S.T. group than in the two groups of mice without *Salmonella* infection (Fig. 1C). The serum IFN-γ concentration of the STZ+S.T. group was lower than the naïve+S.T. group. In addition, the serum IL-6 concentration in the STZ+S.T. group was significantly higher than that in the naïve+S.T. group (Fig. 1C).

H&E staining for the detection of small intestine histopathology 3 days after *Salmonella* infection showed increased infiltration of lymphocytes and plasma cells in the intestinal mucosa of the STZ+S.T. group compared to the naïve+S.T. group, with irregular villi, interstitial edema, vasodilation, and more lymphoplasmacytic infiltration in the small intestine observed under light microscopy. In addition, changes in the adipose tissue around the intestinal wall were observed in the mice, showing more lymphocyte and plasma cell infiltration in the STZ+S.T. group than the naïve-S.T. group (Fig. 1D).

Meanwhile, the results of H&E staining on pancreatic tissue in mice showed that the pancreatic islets of normal mice displayed a scattered distribution, round or oval shape, regular morphology, round islet cells, abundant cytoplasm and round and centered nuclei, while that of diabetic mice presented decreased number, smaller volume, increased nuclear density of islet cells and reduced cytoplasm. No obvious changes were observed in mice with *Salmonella* infection (Fig. 1E). Taken together, the above results demonstrated that accelerated inflammatory progression and increased mortality were found in the hyperglycemic mice infected with *Salmonella*.
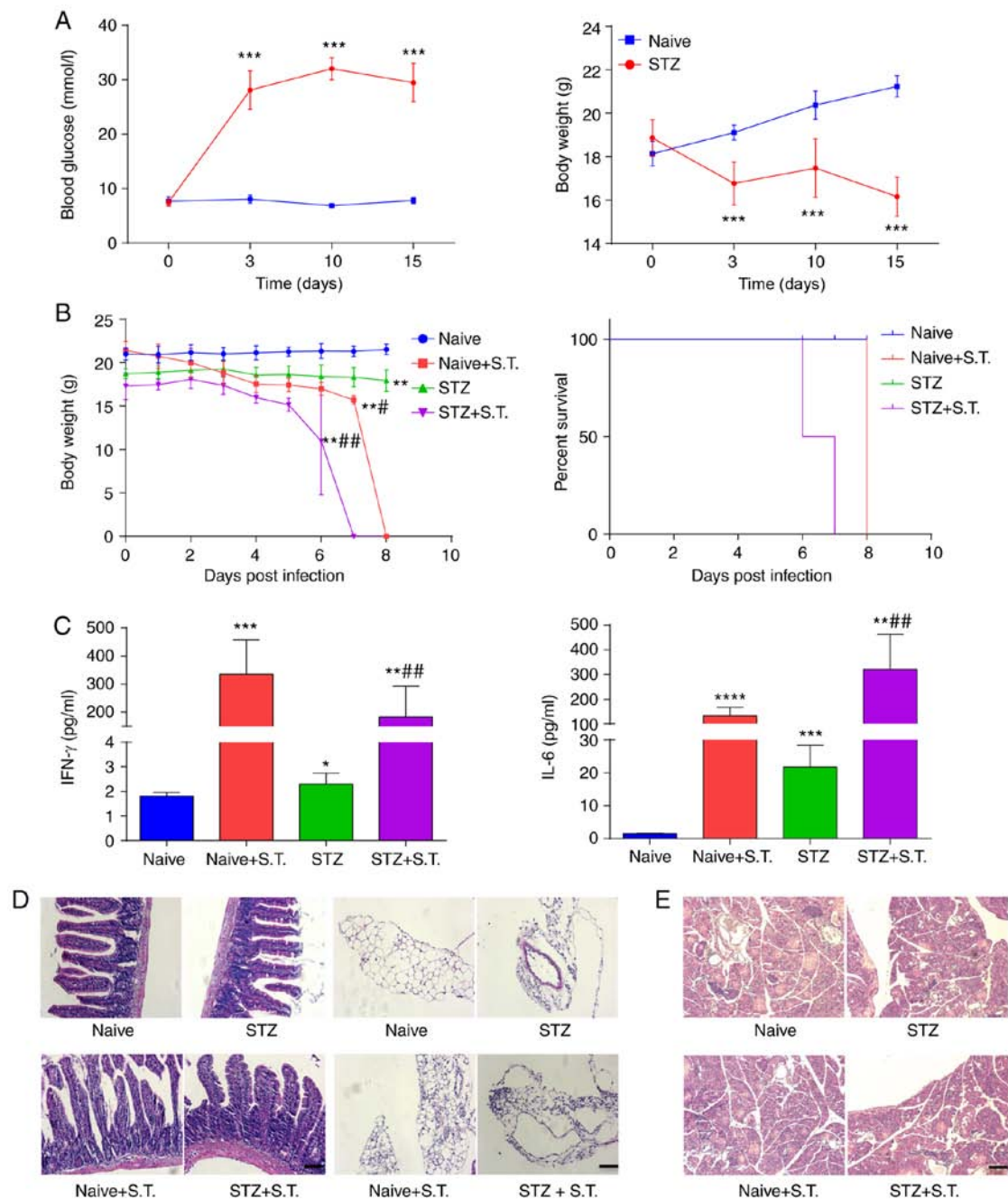
Figure 1. Hyperglycemic mice infected with *Salmonella* show enhanced inflammatory progression and elevated mortality. (A) Continuous monitoring of blood glucose and body weight of mice on days 0, 3, 10 and 15 after the intraperitoneal injection of STZ. (B) Daily monitoring of the body weight and the survival in the hyperglycemic mice 15 days after STZ injection and the control mice after intragastric administration of *Salmonella typhimurium*. (C) ELISA detection of serum IFN-γ and IL-6 levels on day 3 after *Salmonella* infection. (D) H&E staining showing the histology of paraffin-embedded small intestine on day 3 after *Salmonella* infection (scale bar, 50 μm). Inflammatory changes in the intestinal lamina propria and adipose tissue surrounding the intestinal wall were observed. (E) H&E staining showing the histology of paraffin-embedded pancreatic tissue on day 3 after *Salmonella* infection (scale bar, 50 μm). $^*P<0.05$, $^{**}P<0.01$, $^{***}P<0.001$, $^{****}P<0.0001$, compared with the naïve group; $^{\#}P<0.05$, $^{\#\#}P<0.01$, compared with the STZ group (ANOVA). Means ± standard deviation are shown (n=5). STZ, streptozotocin; S.T., *Salmonella typhimurium;* IFN-γ, interferon γ; IL-6, interleukin 6.

Changes in DCs, macrophages, monocytes and neutrophils in the intestinal LP of hyperglycemic mice after Salmonella infection. Three days after *Salmonella* infection, we collected the LP from all of the mice, performed collagenase digestion, and prepared single-cell suspensions to stain with fluorescent antibodies. For the LP, Alexa 430 was used to label the dead cells, and single cells were gated for analysis. Cells with double-positive staining of IA/IE and CD11c were defined as DCs. Cells with Ly6C and CD11b expression were defined

as Ly6C^{hi}CD11b$^+$ monocytes and Ly6C^{int}CD11b$^+$ neutrophils. Cells with F4/80 and CD64 expression were defined as F4/80$^+$CD64$^+$ macrophages. The ratios of DCs and monocytes in the LP of the STZ+S.T. group were significantly lower, and the neutrophil ratio was significantly greater than in the naïve group (Fig. 2A and B).

Changes in the DC subpopulations in the LP of hyperglycemic mice after Salmonella infection. Given the significant
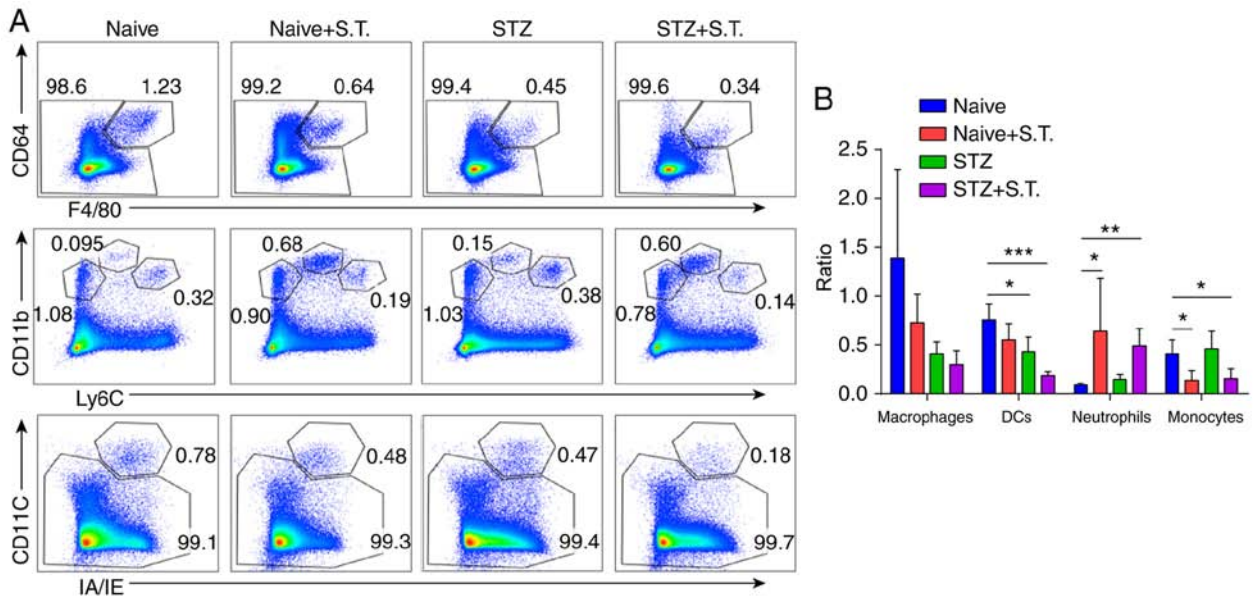
Figure 2. Changes in DCs, macrophages, monocytes and neutrophils in the LP of hyperglycemic mice after *Salmonella* infection. (A) Flow cytometry analysis evaluating the changes in IA/IE+CD11c+ double staining in DCs, Ly6C^{hi}CD11b+ in monocytes, Ly6C^{int}CD11b+ in neutrophils, and F4/80+CD64+ in macrophages of the LP in different groups of mice on day 3 after *Salmonella* infection. (B) Graph constructed using GraphPad PRISM showing the changes in DCs, monocytes, neutrophils, and macrophages in the LP. *P<0.05, **P<0.01, ***P<0.001 (ANOVA). Means ± standard deviation are shown (n=5). STZ, streptozotocin; S.T., *Salmonella typhimurium;* DCs, dendritic cells; LP, intestinal lamina propria.
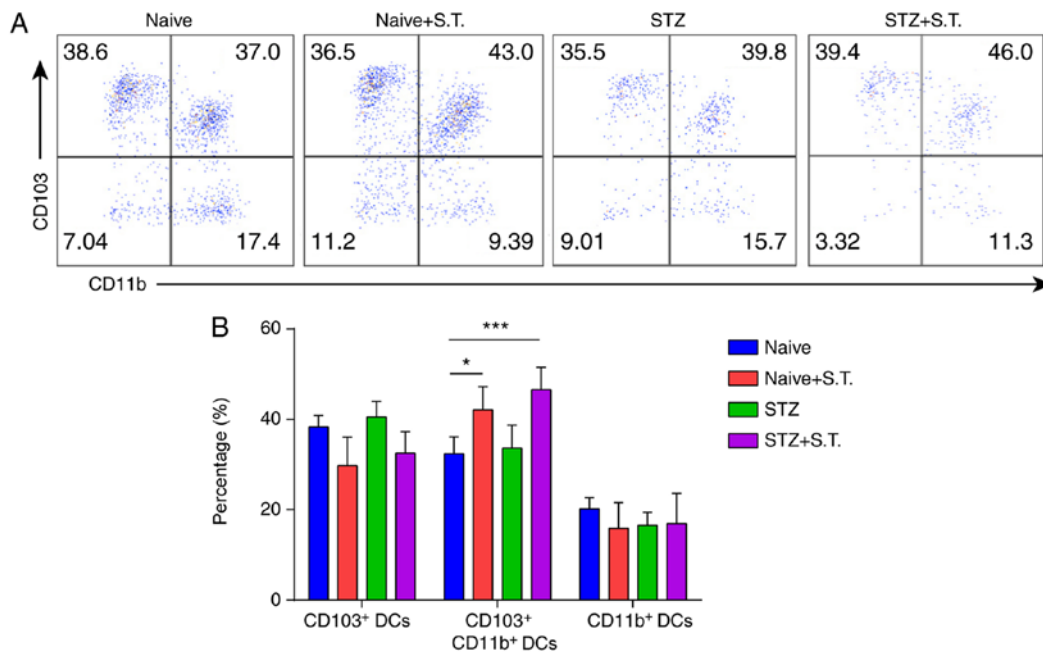

Figure 3. Changes in DC subpopulations in the LP of the hyperglycemic mice after *Salmonella* infection. (A) Flow cytometric analysis showing the changes in the DC subsets in the LP of different groups of mice on day 3 after *Salmonella* infection. (B) Graph constructed using GraphPad PRISM showing the changes in the DC subpopulations, CD103+CD11b- DCs, CD103+CD11b+ DCs and CD103-CD11b+ DCs in the LP. *P<0.05, ***P<0.001 (ANOVA). Means ± standard deviation are shown (n=5). STZ, streptozotocin; S.T., *Salmonella typhimurium;* DCs, dendritic cells; LP, intestinal lamina propria.

reduction of DC ratios in the LP of hyperglycemic mice on day 3 after *Salmonella* infection, we further analyzed the changes in the DC subpopulations and divided the DCs in the LP into CD103+CD11b- DC, CD103+CD11b+ DC and CD103-CD11b+ DC subpopulations according to their CD103 and CD11b expression. The proportion of CD103+CD11b+ DCs was significantly increased in the hyperglycemic mice after *Salmonella* infection, compared with the normal control mice

whereas no significant changes in the other two DC subpopulations were observed in the LP (Fig. 3A and B).

Changes in CD4+FoxP3+ Tregs in the LP and MLN of mice with STZ-induced diabetes after Salmonella infection. On day 3 after *Salmonella* infection, we compared the percentage of CD4+FoxP3+ Tregs in the LP between the STZ+S.T. group and the naïve group and observed a significant increase in the
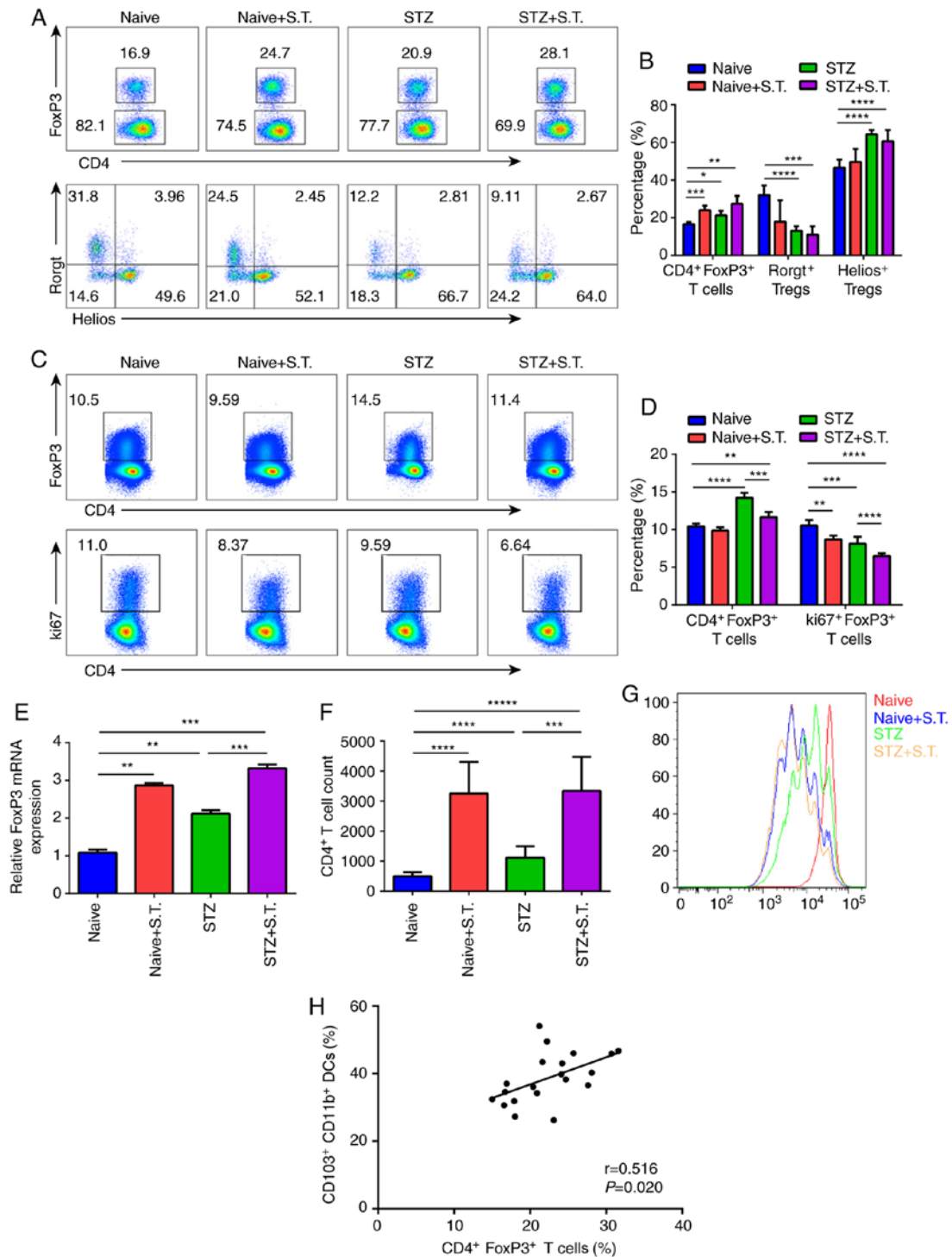
Figure 4. Changes in CD4+FoxP3+ Tregs in the LP and MLN of mice with STZ-induced diabetes after *Salmonella* infection. (A) Flow cytometric analysis showing the changes in CD4+FoxP3+ Tregs in the LP of different groups of mice on day 3 after *Salmonella* infection. The cells were divided into Helios+ Tregs and Rorgt+ Tregs based on their Helios and Rorgt expression. (B) Graph constructed using GraphPad PRISM showing the changes in CD4+FoxP3+ Tregs, CD4+FoxP3+Helios+ Tregs, and CD4+FoxP3+Rorgt+ Tregs in the LP. (C) Flow cytometric analysis showing the changes in CD4+FoxP3+ Tregs in the MLN of different groups of mice on day 3 after *Salmonella* infection; the analysis of Treg proliferation based on ki67 expression. (D) Graph constructed using GraphPad PRISM showing the changes in CD4+FoxP3+ Tregs and ki67+ Tregs in the MLN. (E) mRNA expression of mouse intestinal FoxP3 on day 3 after *Salmonella* infection (n=5). The experiment was repeated 3 times. Means ± standard error of the mean are shown. (F and G) Three days after *Salmonella* infection, we sorted CD103+CD11b+ DCs (5x10^4 cells/well) from the LP and cocultured them with eFlur450-labeled OT-II CD4+ T cells (1x10^5 cells/well) in the presence of OVA$_{323-339}$ (10 μg/ml) for 96 h *in vitro*. The dilution of eFlur-450 in CD4+ T cells was analyzed. The histogram shows the number of CD4+ T cells counted by flow cytometry. (H) Correlation of CD103+CD11b+ DC cells and CD4+FoxP3+ Treg cells. *P<0.05, **P<0.01, ***P<0.001, ****P<0.0001 (ANOVA), *****P<0.00001. Means ± standard deviation are shown (n=5). Tregs, regulatory T cells; STZ, streptozotocin; S.T., *Salmonella typhimurium*; DCs, dendritic cells; LP, intestinal lamina propria; MLN, mesenteric lymph nodes.

percentage of CD4+FoxP3+ Tregs in the LP of the hyperglycemic mice after *Salmonella* infection. Subpopulation analysis

showed that the percentage of Helios+ Tregs was increased, and the Rorgt+ Treg proportion was decreased (Fig. 4A and B).

In contrast, a prominent decline in the CD4+FoxP3+ Treg proportion in the MLN was detected in hyperglycemic mice infected with *Salmonella*, which was caused by affected Treg proliferation due to the decline in the percentage of ki67+ Tregs (Fig. 4C and D).

Consistent with the results of flow cytometry, mRNA expression of FoxP3 (a typical transcription factor of Tregs) was significantly increased in the hyperglycemic mice after *Salmonella* infection (Fig. 4E). Meanwhile, we sorted the CD103+CD11b- DCs, CD103+CD11b+ DCs and CD103-CD11b+ DCs from the LP and cocultured them with CD4+ T cells from OT-II mice. After 4 days, we found that when infected with *Salmonella*, CD103+CD11b+ DCs from STZ-induced diabetic mice could promote the expansion of CD4+ T cells with a stronger efficiency (Fig. 4F and G).

Furthermore, we sorted out CD103+CD11b+ DC cells (Fig. 3) and CD4+FoxP3+ Tregs (Fig. 4A and B), and conducted Pearson correlation analysis on the known data, which showed a positive correlation between the percentage of CD103+CD11b+ DCs and CD4+FoxP3+ Tregs (Fig. 4H; $P<0.05$).

Discussion

Diabetes is characterized by chronic hyperglycemia, which is closely related to the environment of hyperglycemia in the human body. Continuous high glucose increases plasma osmotic pressure, resulting in chemotaxis, adhesion and phagocytosis of immune cells, such as leukocytes and mononuclear macrophages (15). The patient's humoral and cellular immunity decline, and the body's resistance is reduced. Hyperglycemia is also a good medium for bacterial growth and reproduction (16). The chance of infection is not only increased but also difficult to control. In addition, infection puts the human body in a state of stress, and blood glucose reactivity is increased and is difficult to control, thereby aggravating the infection.

The present study evaluated the changes in different immune cells and cell subpopulations in the intestinal LP of hyperglycemic mice after *Salmonella* infection and showed that *Salmonella* infection significantly increased the number of neutrophils in the hyperglycemic mice, which had significant inflammation. In addition, cytokine detection showed that the serum IL-6 concentration was elevated in the hyperglycemic mice after *Salmonella* infection, confirming the above finding. H&E staining for the intestinal histopathology revealed a significant infiltration of inflammatory cells in the intestinal tissues of hyperglycemic mice after *Salmonella* infection. Combined with the mortality data, hyperglycemic mice with *Salmonella* infection died earlier than the C57BL/6 mice with *Salmonella* infection, suggesting that hyperglycemia disrupted immune tolerance and accelerated the occurrence and progression of the bacterial infection.

In this process, we analyzed the changes in the DC subpopulations in the LP and showed that the number of DCs in the LP was reduced in the hyperglycemic mice after *Salmonella* infection. In the LP, the CD103+CD11b+ DC ratio was reduced in the hyperglycemic mice after infection. DCs are a morphologically, structurally, and functionally heterogeneous cell population and a key regulatory component that regulates both intrinsic and adaptive immune responses. DCs are the most potent of the antigen-presenting cells (APCs) (17). They stimulate initial T cell proliferation and play an important role in inducing Treg production (18). The microenvironment of the intestine allows for the regulatory function of DCs in the intestine (19). Experimental evidence has shown that the maintenance of intestinal tolerance depends on DCs. Intestinal DCs capture antigens in different ways (20). CD103- DCs are the major DC subpopulation in the LP that engulf antigens. However, this subpopulation does not stimulate the proliferation of antigen-specific CD4+ T cells *in vitro* (21). The other DC subpopulation in the LP, CD103+ DC, can induce CD4+ T cell proliferation, although this subpopulation has a weaker ability to engulf the antigen than the CD103- DC subpopulation (22,23).

Studies have shown that FoxP3+ Treg function is reduced in type 1 diabetes mellitus (T1DM), but their conclusions are based on the Treg phenotypes found in the peripheral circulation rather than the Treg phenotypes at the site of tissue injury (8). To better understand the loss of immune tolerance in T1DM, the key question that needs to be answered is whether the reduction of the Treg inhibitory effect is due to changes in the immune system caused by the development of T1DM or if Treg dysfunction is involved in disease onset. In this study, the CD4+FoxP3+ Treg ratio in the intestinal LP of the *Salmonella*-infected hyperglycemic group was significantly higher than in the *Salmonella*-infected control group on day 3 after *Salmonella* infection. Additionally, the hyperglycemic mice infected with *Salmonella* presented increased mRNA expression of FoxP3 (a typical transcription factor of Tregs); while without western blot analysis, we could not conclude that the hyperglycemic mice infected with *Salmonella* had more FoxP3. Further analysis of the changes in the subpopulations indicated an increase in the Helios+ Treg ratio and decrease in the Rorgt+ Treg ratio. The increase in the Helios+ Treg ratio may be negative feedback from the inflammatory response in the body while the decrease in the Rorgt+ Treg ratio may lead to an aggravation of intestinal inflammation. These two Treg changes might occur at different times, with the Rorgt+ Treg reducing first to aggravate the inflammation and the Helios+ Treg increasing subsequently to prepare to suppress the aggravation of the inflammation. Moreover, the CD4+FoxP3+ Treg ratio in the mesenteric lymph nodes (MLN) was significantly decreased in hyperglycemic mice after *Salmonella* infection, which was caused by decreased ki67 expression in Tregs after *Salmonella* infection, suggesting a decreased number due to altered Treg proliferation ability. In addition, Boehm *et al* (24) showed that depletion of FoxP3 could promote intestinal inflammatory responses, suggesting that FoxP3 plays an important but complex function during this progress.

We sorted the CD103+CD11b- DCs, CD103+CD11b+ DCs and CD103-CD11b+ DCs from the LP and cocultured them with CD4+ T cells from OT-II mice. We found that when infected with *Salmonella*, CD103+CD11b+ DCs in STZ-induced diabetic mice could promote the expansion of CD4+ T cells with a stronger efficiency. This correlation analysis showed that the elevation of CD4+FoxP3+ Tregs was correlated with the increased number of CD103+CD11b+ DCs in this model. As the only DC subset that presents food protein and bacterial antigens to T cells, intestinal CD103+ DCs have attracted the attention of immunologists due to their functions

in oral tolerance. Distinct from CD103⁻ DCs, these CD103⁺ DCs express high levels of CCR6, CCR7, TLR5 and TLR9, but low levels of costimulatory molecules and inflammatory molecules (25). Chemokines are important regulators in the maintenance of intestinal immune tolerance. CD103⁺ DCs can migrate into the MLN in a CCR7-dependent manner, where they present intestinal antigens to T cells and induce the expression of homing-associated molecules CCR9 and α4β7 on T cells (26). CD103⁺ DCs are the only population that can induce the expression of homing-associated molecules on T cells and B cells in the intestine. The expression of homing-associated molecules CCR9 and α4β7 could help T cells and B cells home back into the intestinal mucosa. Alternatively, CD103⁺ DCs can function by inducing Tregs. CD103⁺ DCs may promote the induction of FoxP3⁺ Tregs by TGF-β and retinoic acid. They may also help IDO catalyze tyrosine and then release hazardous metabolites, thus inhibiting effector T cells and inducing Tregs (27). CD11b⁺ DC could induce the differentiation of antigen-specific naive CD4⁺ T cells into regulatory CD4⁺ T cells by secreting IL-10 and IL-27, which causes oral tolerance (28).

In summary, the Treg ratio in the intestinal LP was elevated, which may be due to the stimulation of antigen-specific CD4⁺ T cell proliferation and their differentiation into FoxP3⁺ Tregs to maintain intestinal homeostasis after CD103⁺CD11b⁺ DC capture of *Salmonella* in the LP. With more in-depth studies on T1DM target organs, Treg-mediated immune regulation in T1DM will be more clearly revealed, providing a fundamental basis for establishing a methodology to treat hyperglycemia-associated infectious diseases. However, additional sample numbers are needed to verify the relationship between CD4⁺FoxP3⁺ Tregs and CD103⁺CD11b⁺ DCs.

Acknowledgements

Not applicable.

Funding

This work was supported by the National Natural Science Foundation of China (grant no. 81172882).

Availability of data and materials

The datasets used and/or analyzed during the current study are available from the corresponding author on reasonable request.

Authors' contributions

SZ conceived and designed the study together with MW and XW. HL and HT were involved in data collection. SZ, MW and XL performed the statistical analysis and prepared the figures. XW drafted the paper. HL and HT contributed substantially to its revision. All authors read and approved the final manuscript.

Ethics approval and consent to participate

This study was approved by the Laboratory Animal Care Committee of Taishan Medical University (Taian, China), and all animal experiments were conducted in accordance with the Guidelines of the Care and Use of Laboratory Animals of Taishan Medical University.

Patient consent for publication

Not applicable.

Competing interests

The authors declare that they have no competing interests.

References

1. Cho NH, Shaw JE, Karuranga S, Huang Y, da Rocha Fernandes JD, Ohlrogge AW and Malanda B: IDF Diabetes Atlas: Global estimates of diabetes prevalence for 2017 and projections for 2045. Diabetes Res Clin Pract 138: 271-281, 2018.
2. Hooper LV and Macpherson AJ: Immune adaptations that maintain homeostasis with the intestinal microbiota. Nat Rev Immunol 10: 159-169, 2010.
3. Vickery BP, Scurlock AM, Jones SM and Burk AW: Mechanisms of immune tolerance relevant to food allergy. J Allergy Clin Immunol 127: 576-586, 2011.
4. Steele-Mortimer O: The *Salmonella*-containing vacuole: Moving with the times. Curr Opin Microbiol 11: 38-45, 2008.
5. Ohkura N, Kitagawa Y and Sakaguchi S: Development and maintenance of regulatory T cells. Immunity 38: 414-423, 2013.
6. Lindley S, Dayan CM, Bishop A, Roep BO, Peakman M and Tree TI: Defective suppressor function in CD4(+)CD25(+) T-cells from patients with type 1 diabetes. Diabetes 54: 92-99, 2005.
7. Putnam AL, Vendrame F, Dotta F and Gottlieb PA: CD4⁺CD25ʰⁱᵍʰ regulatory T cells in human autoimmune diabetes. J Autoimmun 24: 55-62, 2005.
8. Zhang XX, Qiao YC, Li W, Zou X, Chen YL, Shen J, Liao QY, Zhang QJ, He L and Zhao HL: Human amylin induces CD4⁺Foxp3⁺ regulatory T cells in the protection from autoimmune diabetes. Immunol Res 66: 179-186, 2018.
9. Eizirik DL and Mandrup-Poulsen T: A choice of death-the signal-transduction of immune-mediated beta-cell apoptosis. Diabetologia 44: 2115-2133, 2001.
10. Serreze DV, Chapman HD, Varnum DS, Hanson MS, Reifsnyder PC, Richard SD, Fleming SA, Leiter EH and Shultz LD: B lymphocytes are essential for the initiation of T cell-mediated autoimmune diabetes: Analysis of a new 'speed congenic' stock of NOD.Ig mu null mice. J Exp Med 184: 2049-2053, 1996.
11. Salahuddin M, Jalalpure SS and Gadge NB: Antidiabetic activity of aqueous bark extract of Cassia glauca in streptozotocin-induced diabetic rats. Can J Physiol Pharmacol 88: 153-160, 2010.
12. Zenk SF, Jantsch J and Hensel M: Role of *Salmonella* enterica lipopolysaccharide in activation of dendritic cell functions and bacterial containment. J Immunol 183: 2697-2707, 2009.
13. Livak KJ and Schmittgen TD: Analysis of relative gene expression data using real-time quantitative PCR and the 2(-Delta Delta C(T)) method. Methods 25: 402-408, 2001.
14. Voedisch S, Koenecke C, David S, Herbrand H, Förster R, Rhen M and Pabst O: Mesenteric lymph nodes confine dendritic cell-mediated dissemination of *Salmonella* enterica serovar Typhimurium and limit systemic disease in mice. Infect Immun 77: 3170-3180, 2009.
15. Guariguata L, Whiting DR, Hambleton I, Beagley J, Linnenkamp U and Shaw JE: Global estimates of diabetes prevalence for 2013 and projections for 2035. Diabetes Res Clin Pract 103: 137-149, 2014.
16. Bezuglova AM, Konenkova LP, Doronin BM, Buneva VN and Nevinsky GA: Affinity and catalytic heterogeneity and metal-dependence of polyclonal myelin basic protein-hydrolyzing IgGs from sera of patients with systemic lupus erythematosus. J Mol Recognit 24: 960-974, 2011.
17. Steinman RM: Dendritic cells in vivo: A key target for a new vaccine science. Immunity 29: 319-324, 2008.
18. Pulendran B, Tang H and Manicassamy S: Programming dendritic cells to induce T(H)2 and tolerogenic responses. Nat Immunol 11: 647-655, 2010.

19. Bekiaris V, Persson EK and Agace WW: Intestinal dendritic cells in the regulation of mucosal immunity. Immunol Rev 260: 86-101, 2014.
20. Ko HJ and Chang SY: Regulation of intestinal immune system by dendritic cells. Immune Netw 15: 1-8, 2015.
21. Coombes JL and Powrie F: Dendritic cells in intestinal immune regulation. Nat Rev Immunol 8: 435-446, 2008.
22. Schulz O, Jaensson E, Persson EK, Liu X, Worbs T, Agace WW and Pabst O: Intestinal CD103+, but not CX3CR1+, antigen sampling cells migrate in lymph and serve classical dendritic cell functions. J Exp Med 206: 3101-3114, 2009.
23. Jaensson E, Uronen-Hansson H, Pabst O, Eksteen B, Tian J, Coombes JL, Berg PL, Davidsson T, Powrie F, Johansson-Lindbom B and Agace WW: Small intestinal CD103+ dendritic cells display unique functional properties that are conserved between mice and humans. J Exp Med 205: 2139-2149, 2008.
24. Boehm F, Martin M, Kesselring R, Schiechl G, Geissler EK, Schlitt HJ and Fichtner-Feigl S: Deletion of Foxp3+ regulatory T cells in genetically targeted mice supports development of intestinal inflammation. BMC Gastroenterol 12: 97, 2012.
25. Jang MH, Sougawa N, Tanaka T, Hirata T, Hiroi T, Tohya K, Guo Z, Umemoto E, Ebisuno Y, Yang BG, et al: CCR7 is critically important for migration of dendritic cells in intestinal lamina propria to mesenteric lymph nodes. J Immunol 176: 803-810, 2006.
26. Correction to Lancet Diabetes Endocrinol 2018; 6: 186-96. Lancet Diabetes Endocrinol 6: e4, 2018.
27. Matteoli G, Mazzini E, Iliev ID, Mileti E, Fallarino F and Puccetti P: Gut CD103+ dendritic cells express indoleamine 2,3-dioxygenase which influences T regulatory/T effector cell balance and oral tolerance induction. Gut 59: 595-604, 2010.
28. Shiokawa A, Tanabe K, Tsuji NM Sato R and Hachimura S: Hachimura, IL-10 and IL-27 producing dendritic cells capable of enhancing IL-10 production of T cells are induced in oral tolerance. Immunol Lett 125: 7-14, 2009.